HOKKAIDO UNIVERSITY

Title	Vibration testing based on impulse response excited by laser ablation
Author(s)	Kajiwara, Itsuro; Hosoya, Naoki
Citation	Journal of Sound and Vibration, 330(21), 5045-5057 https://doi.org/10.1016/j.jsv.2010.09.036
Issue Date	2011-10-10
Doc URL	http://hdl.handle.net/2115/47242
Type	article (author version)
File Information	JSV330-21_5045-5057.pdf

Instructions for use

Hokkaido University Collection of Scholarly and Academic Papers : HUSCAP

Vibration Testing Based on Impulse Response Excited by Laser Ablation

Itsuro KAJIWARA[#1] and Naoki HOSOYA[#2]

#1 (Corresponding author)
Professor
Division of Human Mechanical Systems and Design, Hokkaido University
N13, W8, Kita-ku, Sapporo 060-8628, Japan
Phone +81-11-706-6390, Fax. +81-11-706-6390
E-mail: ikajiwara@eng.hokudai.ac.jp

#2
Associate Professor
Department of Engineering Science and Mechanics, Shibaura Institute of Technology
3-7-5 Toyosu, Koto-ku, Tokyo 135-8548, Japan
Phone +81-3-5859-8055, Fax. +81-3-5859-8001
E-mail: hosoya@sic.shibaura-it.ac.jp

Abstract:

This paper proposes an innovative vibration testing method based on impulse response excited by laser ablation. In conventional vibration testing using an impulse hammer, high-frequency elements of over tens of kilohertz are barely present in the excitation force. A pulsed high-power YAG laser is used in this study for producing an ideal impulse force on a structural surface. Illuminating a point on a metal with the well-focused YAG laser, laser ablation is caused by generation of plasma on the metal. As a result, an ideal impulse excitation force generated by laser ablation is applied to the point on the structure. Therefore, it is possible to measure high-frequency FRFs due to the laser excitation. A water droplet overlay on the metal is used to adjust the force magnitude of laser excitation. An aluminum block that has nine natural frequencies below 40 kHz is employed as a test piece. The validity of the proposed method is verified by comparing the FRFs of the block obtained by the laser excitation, impulse hammer, and finite element analysis. Furthermore, the relationship between accuracy of FRF measurements and sensitivity of sensors is investigated.

Keywords: Laser Ablation, High Frequency Vibration, Impulse Response, Impact Testing, Frequency Response Function

1. Introduction

In order to obtain the dynamic characteristics of a structure, FRFs (Frequency Response Functions) are obtained by applying an excitation force to the structure and measuring the input/output using a load cell, an accelerometer and so on. The excitation force is generally applied using an impulse hammer or a vibration exciter; in particular, the impact testing using an impulse hammer is used widely for vibration testing due to the simplicity of the apparatus. However, the impact testing relies significantly on the skill and experience of the experimenter; additionally, it does not allow application of an ideal impulse excitation, limiting its use to measurements of low- and mid-frequency regions of under several kilohertz. For this reason, it is difficult to conduct accurate FRF measurements on structures that have natural frequencies in the high-frequency region of tens of kilohertz. Evaluation of the high-frequency vibration is becoming very important for various mechanical systems, for example, it is required for the hard disk and optical disk devices that the high-frequency vibration should be evaluated experimentally and suppressed for enhancing the disk density and servo performance of the devices. Additionally, the development of vibration testing system in the high-frequency region contributes to the construction of experimental models and the validation of FE (Finite Element) models with high-frequency natural modes.

In this paper, a vibration testing analysis method based on non-contact impulse excitation using laser ablation is developed in order to apply excitation force in the high-frequency region to structures. High frequency vibration measurement is significantly important to experimentally identify dynamic characteristics of micro devices such as HDD head actuators or MEMS that have in the high frequency region the natural frequencies of a few tens of kilohertz. This method realizes the ideal impulse excitation force by instantly causing laser ablation by pulse-irradiating a metal surface with a high power YAG laser with its pulse duration of 5 ns. It can also be used for vibration testing of devices during actual operation since excitation can be performed without contact. Laser ablation is a process where high-power laser is focused and irradiated on a solid, thereby rapidly increasing the surface temperature of the solid, explosively releasing atoms, molecules, and their ions etc. [1]. In this method, a pulsed high-power laser is used to trigger instantaneous laser ablation on an irradiated surface in order to obtain an ideal impulse excitation input. Vibration measurement in the high-frequency region is thus made possible.

A method of excitation using a laser [2] and a method of vibration testing using sub-laser ablation [3] have been proposed in the past; however, a study aiming to achieve precise vibration testing in the high-frequency region is not yet conducted. Additionally, although development of a hammer gun [4], an automatic impact excitation apparatus [5] have been examined for the purpose of improving the accuracy of FRF measurements that use the impact testing which relies significantly on the skill and

experience of the experimenter, these are not methods for achieving FRF measurement in the high-frequency region.

In this study, an innovative vibration testing method using laser excitation is proposed and an experimental system is developed to measure FRFs in the high-frequency region. In the vibration experiment with this system, the section to be irradiated is exposed to pulsed high-power YAG laser, and impulse excitation force is remotely applied. Here, measurements are made when the laser is applied directly onto the target section, as well as when a minute water droplet is attached to the measurement surface, and the two measurement results are compared and assessed. Also, the results are compared to those of impact testing using an impulse hammer and finite element analysis, and the effectiveness of this method is examined.

2. Creation of vibration testing system using laser ablation

A vibration testing system, in which pulsed high-power laser is irradiated on a structure in order to achieve FRF measurements in the high-frequency region, is described [6][7].

2.1. Laser ablation

The principle through which non-contact excitation force is generated by laser ablation is described. When a laser beam is irradiated on a metal surface as shown in Fig. 1(a), the laser beam is absorbed by the metal, and atoms, molecules, and their ions are released. These absorb the laser beam and generate high-temperature plasma, and a large quantity of particles (plume) are released from the metal (Fig. 1(a), right side) [1]. The momentum generated when mass Δm is released at velocity v from the metal is represented by Δmv, and this constitutes the impulse. In order to generate a larger excitation force on the structure, a water droplet is attached to the metal surface during laser ablation as shown in Fig. 1(b) [8]. The laser ablation occurs on the metal surface since the laser passes through the water droplet and reaches the metal surface. In addition to the release of particles from the metal surface, the water droplet evaporates due to the rapid increase in temperature of the metal surface, releasing mass ΔM of the water droplet at velocity V. The resulting momentum is $\Delta mv+\Delta MV$, allowing a larger impulse to be obtained (Fig. 1(b), right side). The particles and water vapor are released radially from the metal surface, so the direction of the impulse only comprises the element that is normal to the metal surface. This impulse constitutes the excitation force on the structure.

Laser ablation has been examined for application for propulsion of micro air vehicles [6], and is in practical use in the fields of mechanical processing (hole boring, cutting, etc.) and medicine [1].

2.2. Pulsed laser

A vibration testing system using pulsed high-power laser is shown in Fig. 2. A YAG laser (Continuum Surelite II) with a wavelength of 1064nm, output of 650mJ, and a pulse width of 5ns was installed on an optical bed. In order to enable vibration testing using free support and fixed support on structures of various shapes and sizes, the optical axis of the laser beam was first deflected using a mirror, after which the beam was focused to a spot with a diameter of 2μm using a convex lens to cause laser ablation.

2.3. Measurement of input/output

The method of measuring the excitation force generated by laser ablation and its response is described. As shown in Fig. 3, the excitation force generated by laser ablation is measured by fixing a commercially available load cell (PCB208A03, 22.7g, 2.248mV/N) to the input point of the structure using a stud mount. In order to prevent the load cell from being damaged by laser ablation, an aluminum flat plate of size 13.8mm×13.8mm, thickness 1.5mm, and mass 0.7g was attached to the top surface of the load cell using an adhesive, and laser ablation was triggered on the aluminum plate. For the response, a commercially available accelerometer (ONOSOKKI NP-3211, 0.5g, 1.004mV/(m/s^2)) was attached to the measuring point of the structure using an adhesive. A spectral analyzer (A/D; NI PXI 1042Q, NI-4472B, Software; Catec CAT-System) is used for measuring the excitation forces and acceleration responses, and analyzing the frequency responses of the object structure. The maximum measurement frequency is set to 40kHz in this study. According to specifications, the natural frequencies of the load cell and the accelerometer used in this experiment are over 35kHz and 50kHz, respectively. It was verified by experiment that the natural frequencies of both sensors are sufficiently higher than the maximum measurement frequency of 40kHz.

The amplitude of the excitation force can be adjusted by using the evaporation of the water droplet attached on the aluminum plate. The quantity of the water droplet was controlled using a precision dropper (High Tech lab, L1004614).

3. FRF measurement by laser excitation

Effectiveness of FRF measurement in the high-frequency region was assessed by taking vibration measurements under a variety of conditions in terms of the quantity of the water droplet attached to the surface of the target object and the sensitivity of the sensors, based on impulse excitation using the pulsed YAG laser. We focus on FRF in high frequency range, especially between 20 and 40kHz.

3.1. Selection of target structure

As a structure having natural frequencies in the high-frequency zone, a rectangular cuboid aluminum block shown in Fig.4, with dimensions 150mm×50mm×20mm and mass 398g, whose first natural

frequency is 4174Hz, was used as the test piece. In this paper, the out-of-plane modes of the block was considered for the vibration measurement, with two excitation points (points 1 and 2) and three measurement points (points 1, 2, and 3).

3.2. Making of an FE model

An FE model of the block was made in order to compare and assess the accuracy of the FRFs measured using laser excitation with the FRFs obtained by the FEM. The description of the FE model is as follows: quadratic tetra solid elements (mesh size 2.5mm), number of nodes: 47136, number of elements: 29571. In the model, the load cell was taken into account as a rigid body element, and the accelerometer as a point mass element; however the screw holes for mounting the load cell were not taken into account. The reason why both sensors are modeled as rigid mass element is because it was demonstrated that their resonance frequencies are sufficiently higher than the maximum measurement frequency of 40kHz. NASTRAN was used in this paper to conduct an eigenvalue analysis of the block. The natural frequencies of the block obtained with and without the load cell are shown in Table 1. Nine natural frequencies exist under the frequency range of 40kHz and Fig. 5 shows a part of the out-of-plane modes obtained by FE analysis when the load cell is installed on the block. A modal damping ratio of 0.5% was used when calculating the FRFs using FEM. It is confirmed from Figs. 5(b) and (c) that the 2nd and 3rd modes are the local modes at the load cell. We also performed an FE analysis using hexagonal brick elements having an approximately the same degree of freedom and compared the results with the results of the analysis that used quadratic tetra solid elements, and found no significant difference between the two.

3.3. FRF measurements

Using the block shown in Fig. 4, auto-FRFs H_{11} and H_{22} and a cross-FRF H_{31} were measured where points 1 and 2 are the excitation points and points 1, 2, and 3 are the measurement points. H_{ij} is FRF between an input point j and output point i. The aluminum plate was mounted, using an adhesive, on the load cell, which was in turn fixed to the top surface of the block using screws, and the accelerometer was fixed to the bottom surface of the block using an adhesive (see Fig. 3). The aluminum plate is adhered onto the load cell via a large surface with an area ratio of approximately 55%, and is restrained by this surface. Therefore, the natural frequency of the aluminum plate is extremely high and its vibration doesn't influence the measured response. The input and output thus obtained were used to measure the FRFs. Because momentum from evaporation of a water droplet, as well as from the laser ablation, is used as an excitation force during FRF measurements, a 10μℓ water droplet was attached to the aluminum plate and irradiated with pulsed laser. It is confirmed that the excitation force due to laser excitation is highly reproducible and extremely stable.

The averaging count for the FRF measurement is set to 10. Although the aluminum plate mounted on

the load cell suffers wear with increasing number of laser ablations (the number of pulsed laser irradiation during laser excitation), it is confirmed that an excitation count of about 300 does not affect the FRF measurements. Therefore, the aluminum plates were exchanged in this experiment after a rough target of 100 laser excitations.

3.4. Accuracy of FRFs obtained by laser excitation

The accuracy of FRFs in the high-frequency region obtained via this method is assessed by comparing FRFs measured by laser excitation with FRFs obtained through the FEM.

Figure 6 shows the measured excitation force by laser excitation, where Fig. 6(a) shows the time response of the excitation force measured by the load cell, and Fig. 6(b) shows its power spectrum. The figures show that laser ablation using the pulsed high-power YAG laser results in an ideal impulse excitation input which is nearly constant in the measurement target frequency region. Several peaks can be observed in Fig. 6(b); these are thought to be as a result of the inputs measured by the load cell being affected by the dynamic characteristics of the structure. It is also observed from Fig. 6(b) that the natural frequency of the load cell is over the frequency range of 40kHz.

Figures 7, 8 and 9 show the auto-FRF H_{11} at point 1 of the block, the auto-FRF H_{22} at point 2, and the cross-FRF H_{31} between points 3 and 1, with FRFs measured using laser excitation and FRFs obtained through the FEM shown together for comparison. These figures show that both measured and calculated FRFs agree well in the high-frequency region, for both auto-FRF and cross-FRF. The figures also show good coherence in the high-frequency region. Looking at both FRFs in the 10-15kHz region, the number of resonance peaks match, but the shapes of the FRFs do not correlate much. As a result of a detailed investigation with regards to the mismatch between the analysis results and the experimental results in the 10-15kHz frequency band, it has been confirmed that local modes at the load cell exist in this region, and that the tightening torque of the load cell has a significant effect. The local modes at the load cell are shown in Fig. 5(b) and (c). Namely, the tightening torque of the load cell has a strong effect on rigidity and damping caused by friction of the screw contact section, and such characteristics are difficult to replicate using FEM. However, since the calculated results and the experimental results correlated well in the high frequency region, especially in the region over 20kHz of the target frequency range, the FEM model is considered to be thoroughly appropriate for this analysis. Through an eigenvalue analysis using FEM, it is confirmed that there is no local mode at the load cell between 20-40kHz as shown in Table 1 and the resonance peak observed near the 25kHz mark in the laser excitation FRF is an in-plane vibration mode measured by the crosstalk of the accelerometer. It is also confirmed from Figs.7, 8 and 9 that the sensors' own resonances of the load cell and accelerometer don't influence the measured FRFs.

If we conduct the above-mentioned FE analysis, we can forecast the existence of the local modes at the load cell in a specific frequency region. An experimental approach to specify the local modes is to experimentally identify the natural modes of the structure by experimental modal analysis. But, it is very difficult to control the frequencies of the local modes. A solution of the load cell attachment problem is to analyze the frequency response function by only measuring the output data without using the load cell. Figure 10 shows the power spectrum of the accelerometer output data at point 1. The input force by the laser excitation is almost ideal impulse and so the shape of the output power spectrum in Fig. 10 corresponds well with the amplitude of the frequency response function in Fig.7. If we can estimate the size of the input force and the time when the input force is applied, the frequency response function can be analyzed by only measuring the output data without using the load cell. Now, the authors are evaluating this methodology and the latest results will be submitted to this journal as a sequel to this study in near future.

3.5. Comparison with FRF using impact testing

The accuracy of FRF is examined by comparing the FRF measured by laser excitation and the FRF measured by the impact testing. Figures 11, 12 and 13 show the auto-FRF H_{11} at point 1 of the block, the auto-FRF H_{22} at point 2, and the cross-FRF H_{31} between points 3 and 1, with FRFs measured by laser excitation and FRFs measured by the impact testing shown together for comparison. In order to ensure that the measurement conditions of the FRFs using laser excitation and the impact testing are identical, the excitation force due to impact of the impulse hammer was measured using the same load cell for the laser excitation measurement. Figures 11, 12 and 13 show that the FRFs using both methods are in close agreement in the frequency region of under 10kHz. However, it can be seen that the coherence of the FRF via the impact testing drops considerably in the frequency region of over 20kHz. Figure 14 shows the difference of input characteristics between the laser and impulse hammer excitations. It is observed from Fig. 14(b) that the power spectrum with the impulse hammer also drops considerably over 20kHz, resulting in the degradation of the accuracy of FRF.

It can also be seen that coherence of the FRF using laser excitation drops in the frequency region of under 1kHz. Figure 15 shows a close-up of auto-FRF H_{22} at point 2 for both methods in the frequency region of under 2kHz. These FRFs are represented by $a/F=1/M$ due to Newton's Second Law, where the mass of the block is M, the excitation force is F, and the acceleration is a. The mass of the block used in this experiment is 398g, so the amplitude of the FRFs is 2.51. The figure shows small, periodical peaks in the FRF via laser excitation, which is different to the FRF obtained by the impact testing. In order to increase the accuracy of measurement in the low frequency region, it is necessary to select appropriate load cell sensitivity and to apply an impulse that can sufficiently excite the modes in the low frequency region. The pulse laser used in this experiment has a pulse width of 5 ns, so it is possible that insufficient impulse was being applied in order to sufficiently excite the vibration in the

low frequency region. Amplification of the input force is an issue which requires further investigation.

3.6. Quantity of the water droplet and accuracy of the FRFs

The relationship between changes in the quantity of the water droplet and FRF accuracy during laser excitation is explained. The relationship between the presence of the water droplet and FRF accuracy will also be examined.

3.6.1. Difference between water droplet quantities of 10μℓ and 20μℓ

Figure 16 shows the auto-FRF H_{11} at point 1 with a water droplet of quantity 10μℓ and a water droplet of quantity 20μℓ, shown together for comparison. Figure 16 shows that both FRFs are in good correlation at all frequency regions, although the coherence of the FRF with a water droplet of quantity 20μℓ is somewhat better than the FRF with a water droplet of quantity 10μℓ. The input force property with a water droplet of quantity 20μℓ is close to Fig. 14 with a water droplet of quantity 10μℓ, however the force amplitude is a bit increased in case of 20μℓ. It is thought that there is an optimum quantity of the water droplet in order to obtain a more accurate FRF in the high-frequency region, in terms of the power of the laser and the amplitude of the excitation force generated.

3.6.2. Accuracy of the FRF depending on the presence of the water droplet

Figure 17 shows the auto-FRF H_{22} at point 2 measured with and without a water droplet of quantity 10μℓ, shown together for comparison. It can be seen that the accuracy of the FRF measured without a water droplet falls significantly in all frequency regions. We can say that attaching a water droplet during laser ablation results in evaporation of the water droplet and a larger excitation force, thus contributing to a relative improvement to the signal-to-noise ratio. We have also found that attaching a water droplet during laser excitation allows the amplitude of the excitation force to be adjusted.

3.7. Load cell sensitivity during FRF measurement

The effect of load cell sensitivity on the accuracy of FRF measurement is discussed. In the previous section, we showed that a greater excitation force can be generated by attaching a water droplet, and that there is an optimum water droplet quantity for high-accuracy FRF measurement in the high-frequency region. In this section, we aim to improve the relative signal-to-noise ratio by using a high-sensitivity load cell, and examine the relationship between the accuracy of FRF measurements and load cell sensitivity. Table 2 shows the sensitivities of load cells examined in this paper. Load cell (a) is a low-sensitivity load cell with which sufficiently accurate FRF measurements were obtained, and load cell (b) is the high-sensitivity load cell to be assessed.

Figure 18 shows the auto-FRF H_{22} at point 2 measured with a water droplet of quantity 10μℓ, where FRFs obtained by the (a) low-sensitivity load cell and the (b) high-sensitivity load cell are shown

together for comparison. It can be seen that the FRF accuracy and coherence of load cell (b) is dramatically lower than those of load cell (a).

The cause of this drop in FRF measurement accuracy is examined using the time response of excitation force obtained by laser excitation. Figure 19 shows the excitation force obtained by laser excitation measured using the (a) low-sensitivity load cell and the (b) high-sensitivity load cell, shown together with the excitation force obtained using an impulse hammer for comparison. It can be seen that the excitation force (a) is a more ideal impulse excitation force in comparison to the excitation force (b) and the impulse hammer excitation. It is observed that the excitation force (b) is not an impulse excitation force, in contrast to the excitation force (a). This undesirable excitation force (b) is considered to be a result of an overload of the load cell. Thus, the inaccuracy of the FRF measurement is also caused by the overload of the load cell. A large impulse force is instantaneously applied to the structure since the pulsed high-power laser is irradiated in very short pulse duration. As a result, a high sensitivity load cell easily causes the overload due to the pulsed laser irradiation. In such an instance, the load cell output is physically meaningless, and the resulting FRFs measured using the load cell is inaccurate. Although an overload is not thought to be present in the accelerometer in this experiment, it is likely that an overload will similarly occur if an accelerometer with a higher sensitivity is used. Accordingly, highly accurate FRF measurements using laser excitation can be made by selecting appropriate sensitivity levels for the load cell and the accelerometer.

4. Conclusions

An innovative vibration testing system that uses a high-power YAG laser to cause laser ablation was developed in order to generate a non-contact and ideal impulse excitation input. Although this method uses a pulsed laser, input and output measurements are taken using commercially available load cells and accelerometers, so this method is roughly the same as regular vibration testing analysis methods. In order to prevent the load cell from damage due to laser ablation, we introduced a technique in which an aluminum plate is mounted on the load cell, wherein the pulsed YAG laser is applied to the aluminum plate. It was shown that it is important to attach a water droplet of an appropriate quantity onto the laser target section in order to obtain a highly accurate FRF during an FRF measurement during laser excitation. In addition, it is necessary to select a load cell and accelerometer with appropriate sensitivities, because the excitation force from laser excitation may cause an overload of the load cell or the accelerometer. Occurrence of overload during FRF measurements depends on the size of the structure, positions of the excitation points or measurement points, and mounting method or sensitivities of the load cell and the accelerometer. We applied this method on a structure having natural frequencies in the high-frequency region, and made comparisons between the FRF measured through laser excitation, the FRF obtained using FEM, and the FRF obtained using a conventional

impact testing method, thereby demonstrating that it is possible to take highly accurate FRF measurements in the high-frequency region, which had not been possible using conventional vibration testing methods. Furthermore, it was also confirmed that coherence property in the high-frequency region is significantly improved in comparison to conventional methods.

Future task of this study includes assessment and amplification of the generated force using a variety of materials including water droplet. There is presently a limit to the size of the excitation force that can be generated using laser ablation, resulting in the restriction of the application to large devices and the measurements in the low frequency range of up to 1kHz. With regards to the material of the irradiated surface, the size of the force with some metals such as aluminum, copper and steel was evaluated, and it is confirmed that a force of equivalent size is generated. However, in order to put the technique to actual use, there is a need to perform tests and assessments using a variety of materials including non-metals and systematize the relationship between the material and the size of the generated force. Another future task of this study for solving the load cell attachment problem is to establish the methodology of input sensorless FRF measurement as described in 3.4.

Acknowledgement

The supports by Japan Society for the Promotion of Science (JSPS) through Grants KAKENHI-A-22246027, and the Ministry of Education, Culture, Sports, Science and Technology (MEXT) in Japan through Grants KAKENHI-A-22686025 are gratefully acknowledged.

References

[1] The institute of Electrical Engineers of Japan ed., *Laser ablation and applications*, 1999, Corona Publishing Co., LTD.
[2] Koss, L. L. and Tobin, R. C., Laser Induced Structural Vibration, *Journal of Sound and Vibration*, Vol.86(1), 1983, pp.1-7.
[3] Philp, W. R., et al, Single Pulse Laser Excitation of Structural Vibration Using Power Densities Below The Surface Ablation Threshold, *Journal of Sound and Vibration*, Vol.185(4), 1995, pp.643-654.
[4] PCB International Corp., *Electric Impact Hammer Operating Guide*, Model 086C.
[5] Iwahara, M., et al., Improvement of Accuracy and Reliability of Experimental Modal Analysis (Invention on Impact Testing and Decrease of Measurement Error), *Transactions of the Japan Society of Mechanical Engineers*, *Series C*, Vol.64, No.618, 1998, pp.538-545.
[6] Obata, T. and Kajiwara, I., A New Method of Vibration Test Using Laser Ablation, *JSME*

Proceedings on Dynamics and Design Conference 2007, 2007, CD-ROM (No.803).
[7] Hosoya, N. and Kajiwara, I., Vibration Testing by Using Laser Ablation, *JSME Proceedings on Dynamics and Design Conference* 2008, 2008, CD-ROM (No.455).
[8] Kajiwara, I., et al., Integrated Laser Propulsion/Tracking System for Laser-Driven Micro-Airplane, *Theoretical and Applied Mechanics Japan*, Vol.53, 2004, pp.115-124.

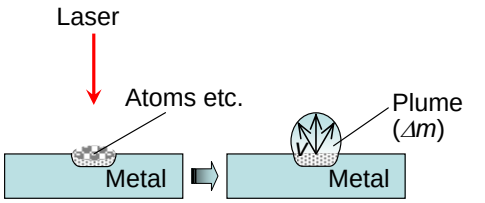

(a) Laser ablation without water droplet

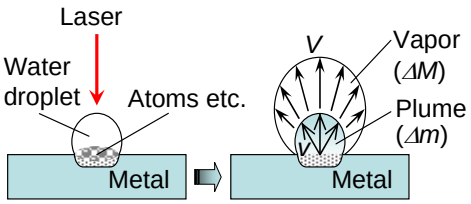

(b) Laser ablation with water droplet

Fig. 1 Excitation force generated by laser ablation

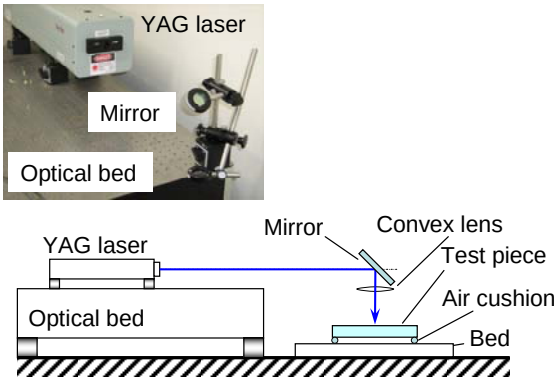

Fig. 2 Experimental system

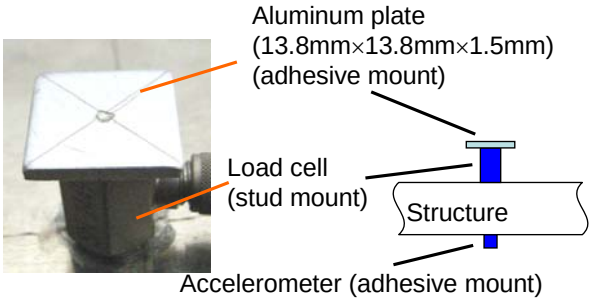

Fig. 3 Attachment of a load cell and an accelerometer

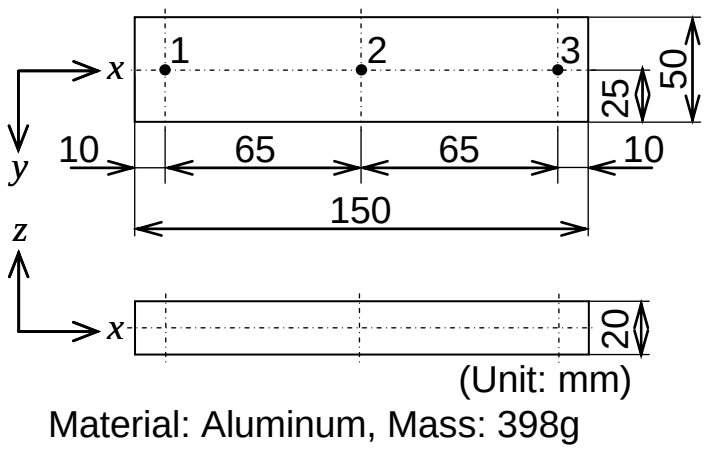

Fig. 4 Excitation and measurement points

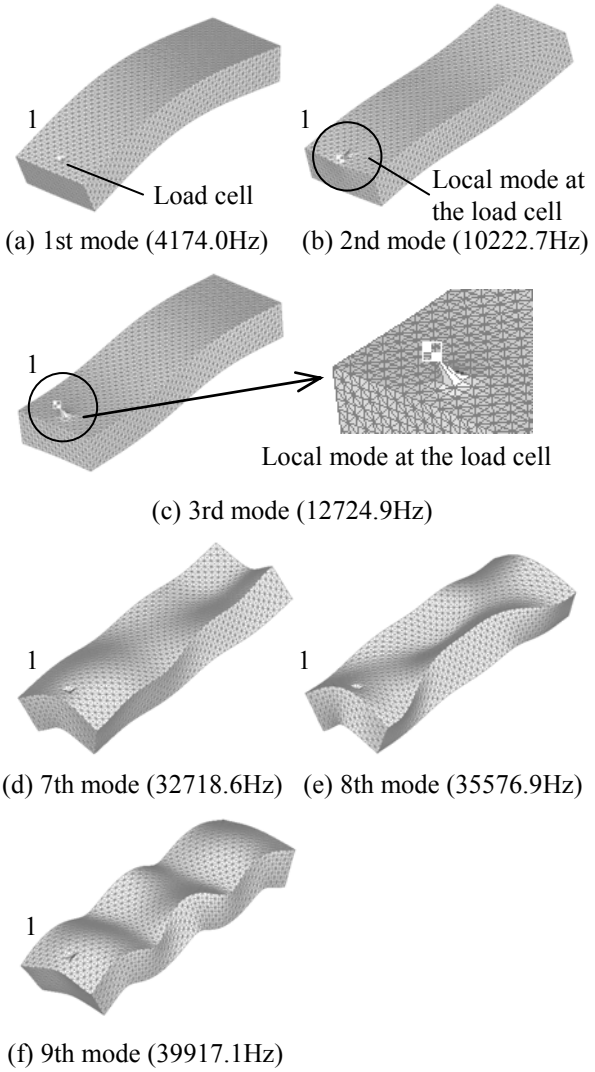

Fig.5 Mode shape of the aluminum block (load cell: point 1)

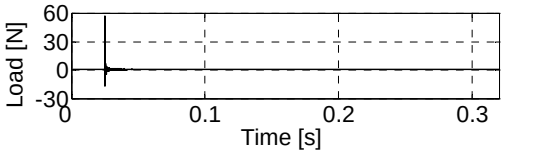

(a) Time response of force

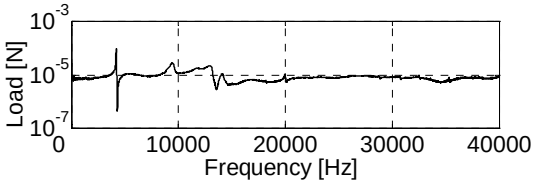

(b) Power spectrum of force

Fig. 6 Measured force by laser excitation

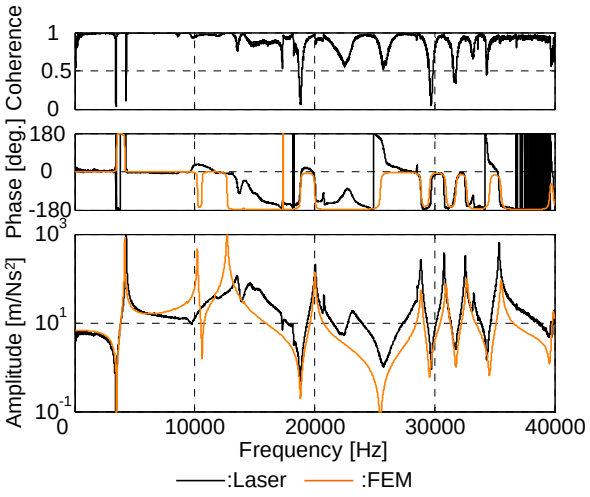

Fig. 7 Auto-FRF H_{11} by laser excitation and FEM

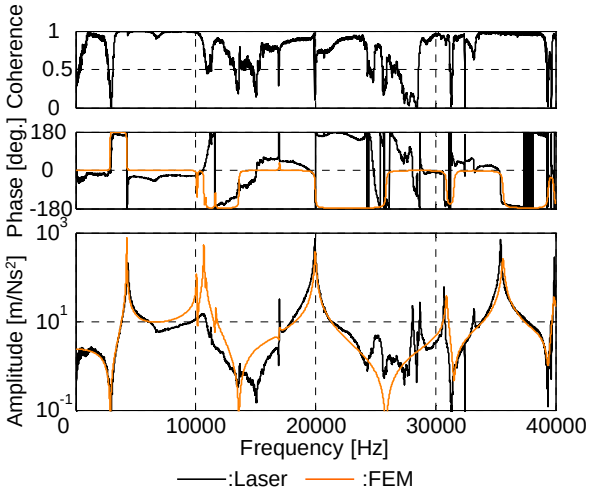

Fig. 8 Auto-FRF H_{22} by laser excitation and FEM

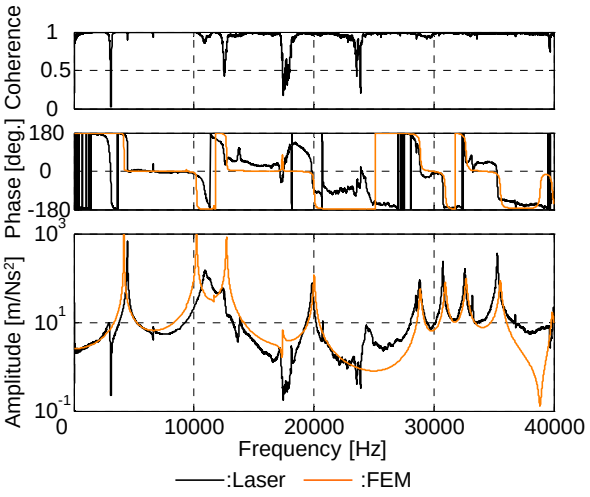

Fig. 9 Cross-FRF H_{31} by laser excitation and FEM

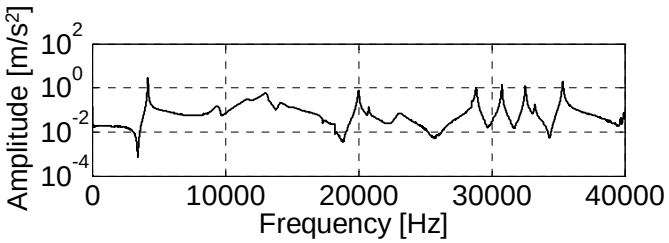

Fig. 10 Power spectrum of the accelerometer output at point 1

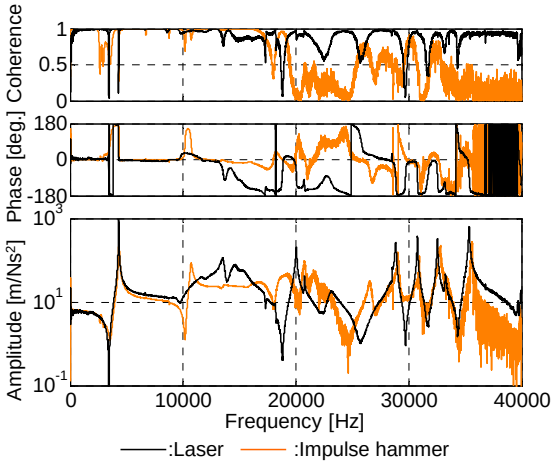

Fig.11 Auto-FRF H_{11} by laser excitation and impulse hammer

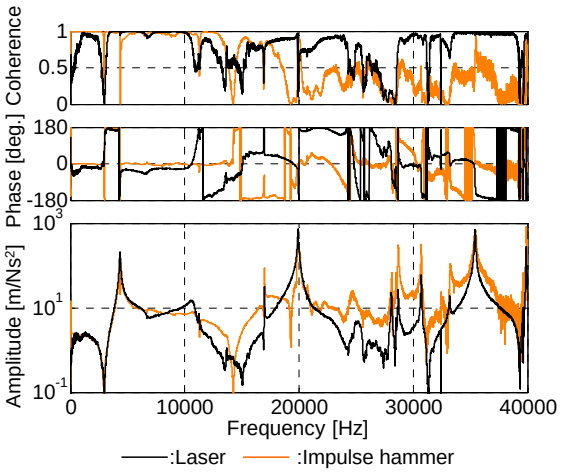

Fig.12 Auto-FRF H_{22} by laser excitation and impulse hammer

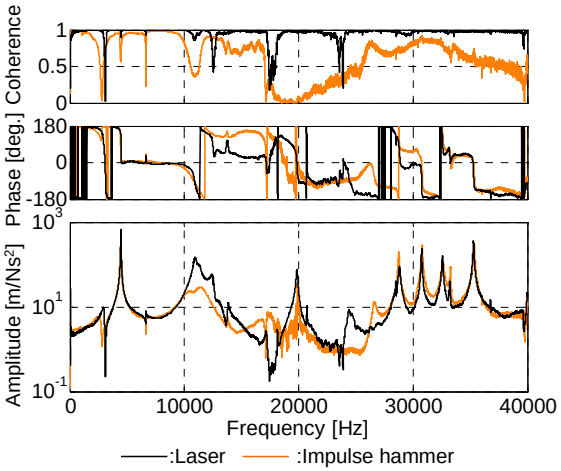

Fig.13 Cross-FRF H_{31} by laser excitation and impulse hammer

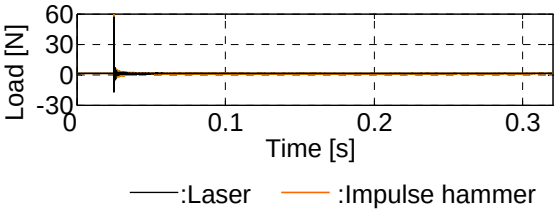

(a) Time response of force

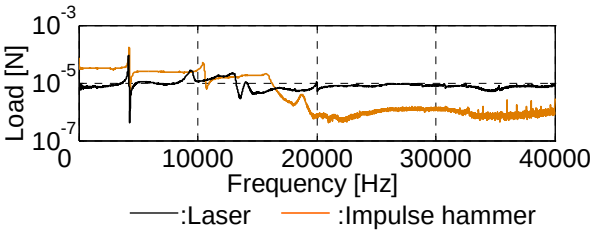

(b) Power spectrum of force

Fig.14 Difference of input characteristics between laser and impulse hammer excitations

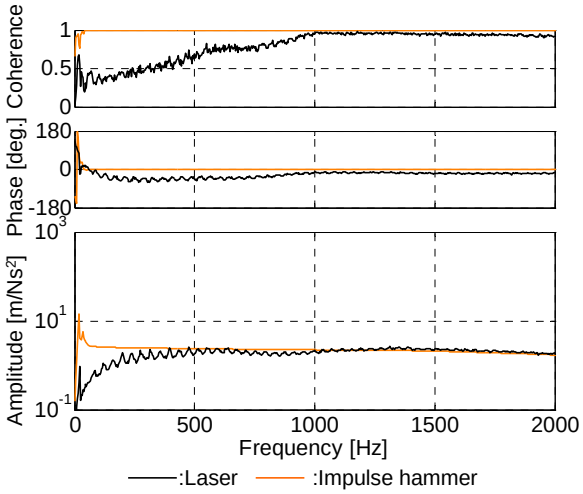

Fig.15 Close-up of auto-FRF H_{22} (0-2kHz)

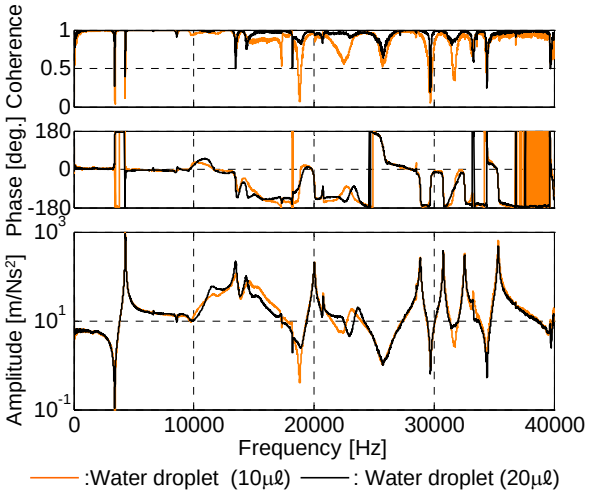

Fig.16 Auto-FRF H_{11} with water droplet 10μℓ and 20μℓ

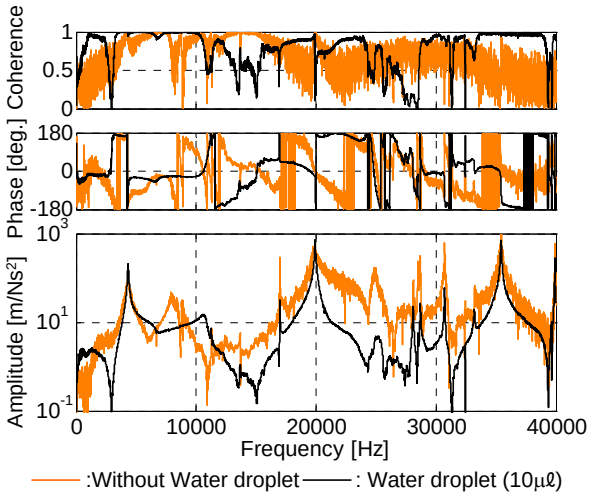

Fig.17 Auto-FRF H_{22} with water droplet 10μℓ and without water droplet

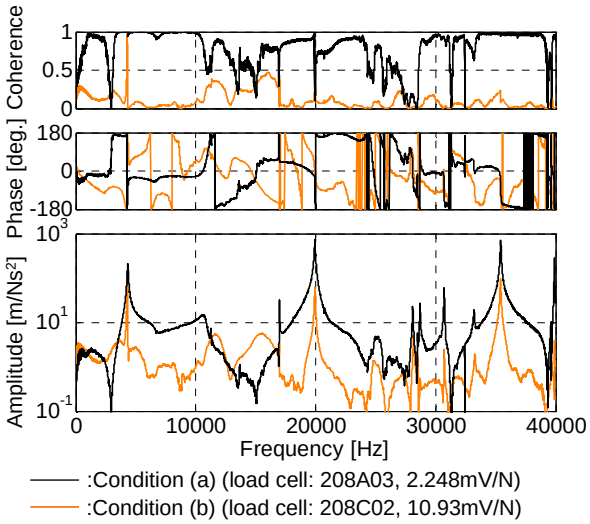

Fig. 18 Auto-FRF H_{22} by condition (a) and (b)

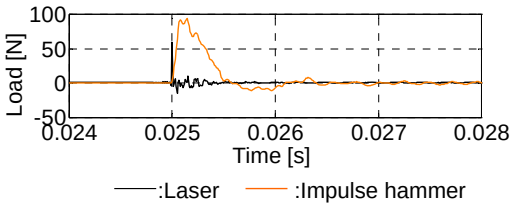

(a) Excitation force by laser excitation (Load cell (a)) and impulse hammer

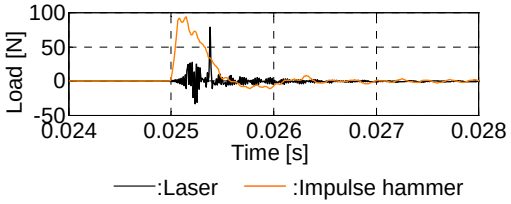

(b) Excitation force by laser excitation (Load cell (b)) and impulse hammer

Fig. 19 Time histories by laser excitation and impulse hammer

Table 1 Natural frequencies of the aluminum block with and without the load cell

With load cell		Without load cell	
Order	Frequency [Hz]	Order	Frequency [Hz]
1st	4174.0	1st	4431.8
2nd	10222.7	2nd	11174.7
3rd	12724.9		
4th	20040.8	3rd	19701.7
5th	28890.6	4th	28741.5
6th	30983.1	5th	30920.0
7th	32718.6	6th	32649.3
8th	35576.9	7th	35499.5
9th	39917.1	8th	39897.3

Table 2 Experimental conditions

	Load cell		Water droplet [μℓ]	Laser output [mJ]
	Type	Sensitivity [mV/N]		
(a)	208A03	2.248	10	650
(b)	208C02	10.93	10	650